The 2010 IEEE/RSJ International Conference on
Intelligent Robots and Systems
October 18-22, 2010, Taipei, Taiwan

On Internal Models for Representing Tactile Information

Giorgio Cannata, Simone Denei, Fulvio Mastrogiovanni

Abstract— **In this paper a framework for representing tactile information in robots is discussed. Control models exploiting tactile sensing are fundamental in social Human-Robot interaction tasks. Difficulties arising in rendering the sense of touch in robots are at different levels: both representation and computational issues must be considered. A layered system is proposed, which is inspired from tactile sensing in humans for building *artificial somatosensory maps* in robots. Experiments in simulation are used to validate the approach.**

I. INTRODUCTION

Robots exploiting tactile information are expected to exhibit advanced capabilities in physical and social Human-Robot Interaction (HRI in short). The sense of touch is a fundamental feature for control models based on physical interaction cues. Appropriate social and physical stimuli are needed to enhance the quality of the interaction in terms of robot behaviour and responsiveness.

To date, studies in HRI have been largely devoted to investigate suitable models for modulating interaction behaviours at the social level [17]. Aspects related to physical interaction received considerable attention mostly with respect to *tactile sensing*, and specifically to transduction technologies [5]. Although the need arises to integrate information from both physically and socially oriented models of interaction, the direct use of tactile data in designing control strategies enforcing social interaction rules did not receive considerable attention in literature.

One possibility is to design appropriate representation structures to mimic *somatosensory* mapping in humans. From one side, these structure must guarantee an *unique* mapping between the tactile elements on the robot surface and their representation; from the other side, they must be accessible from high level behaviours implementing social models of interaction. During the past few years, a number of approaches have partially addressed these key issues. A model aimed at translating contact phenomena into language like symbols has been presented in [23], where the focus is more on the relationship between numerical and symbolic data rather than in the use of such information at the control level. The work presented in [15] faces the problem of the emergent behaviour through sensory-motor interaction between an agent capable of full body movements and the surrounding environment. A somatosensory map is obtained by correlating signals from tactile sensors distributed over the agent surface. A similar approach, based on *Information Theory*, has been proposed in [20], where *sensoritopic maps* of groups of sensors are created using self-organizing processes. Feedback from groups of tactile sensors has been used in [19] to determine sensoritopic connections between correlated taxels: a mostly manual learning process is used to activate groups of nearby taxels, which are then considered *topographically* close to each other.

Both *representation* and *computational* issues must be considered when designing *artificial somatosensory maps*:

- Designing internal models for representing tactile information is a novel research attempt. Differently from vision images, *tactile images* can not be easily *flattened* on a 2D metric space, since they originate from elements that are located on curved surfaces. Such concepts as proximity, feature extraction or data filtering can not be easily applied. Furthermore, cameras provide information from a well-defined location in space, whereas taxels are distributed over large parts of the robot surface, which are subject to kinematics constraints. *A natural representation preserving skin topology must be available.*
- Data structures must guarantee an easy access to a semantically well-defined tactile information. Tactile data at different resolution must be accessible according to the task at hand: high resolution tactile images are needed for fine contact dynamics, whereas reactive behaviours can be attained by manipulating low resolution information with an associated negligible computational load. *The characteristics of the contact must be accessible from the representation.*

Approaches in the literature do not maintain the mapping between the location of taxels in 3D space and their representation in the artificial somatosensory maps. This is fundamental to use tactile data in practice, e.g., when reacting to sudden contacts. The main contribution of this work is a model of somatosensory maps addressing representation issues, which is loosely inspired by tactile rendering in humans. However, it also paves the way for further developments on the computational side, which are outside the scope of the present discussion. Inspired by the beautiful images of [24], a hierarchical architecture for tactile rendering is proposed that exploits *Surface Parameterization* techniques to model somatosensory maps.

The paper is organized as follows. Section II describes the actual tactile information processing *architecture* in humans.

All the authors are with the Department of Communication, Computer and System Sciences, University of Genova, Via Opera Pia 13, 16145, Genova, Italy. Corresponding Author email:fulvio@dist.unige.it.

The research leading to these results has received funding from the European Community's Seventh Framework Programme (FP7/2007-2013) under grant agreement n. 231500/ROBOSKIN.

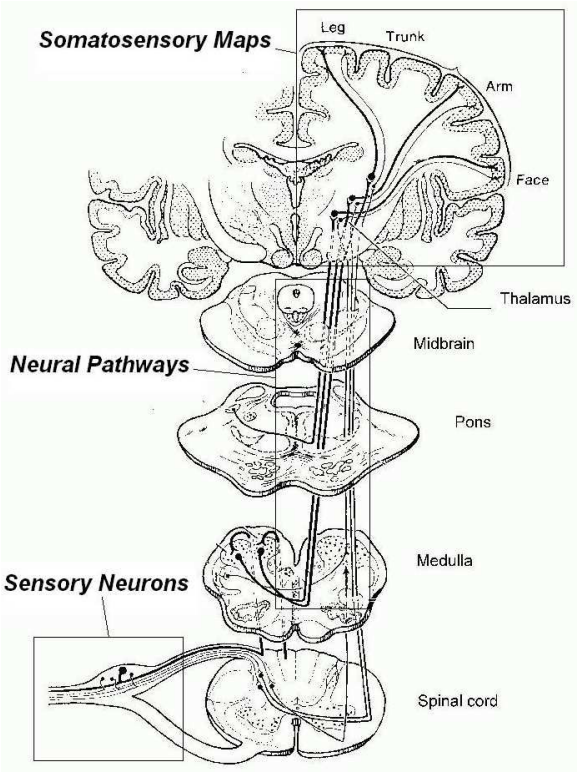

Fig. 1. Somatosensory pathways from sensory neurons to brain maps.

The description is neither exhaustive nor detailed: on the contrary, the aim is to survey few concepts leading to practical design principles for a tactile representation framework. Next, Section III introduces a possible approach to implement artificial somatosensory maps taking representation issues into account. Examples validating the approach are discussed in Section IV. Conclusions follow.

II. Tactile Information Processing in Humans

Nowadays, it is common to discuss *sensory systems* referring to internal models related to the physical arrangement of somatosensory neural pathways at the cortical level [13], [5]. From a general overview of such an architecture it is possible to devise important guidelines to design frameworks for representing tactile data in robots.

In very abstract terms, a sensory system results from the aggregation of functional modules, which are organized in layers (see Figure 1):

- A number of mechanoreceptors distributed throughout the body, which are responsible for transducing physical stimuli into neural signals for afferent *sensory neurons*.
- *Neural pathways* conveying signals from sensory to higher level populations of neurons: early processed signals are directly related to stimuli information, whereas later processing stages are progressively more abstract.
- A number of functionally organized *brain areas* (i.e., different maps) responsible for processing in a highly distributed way the information transmitted through neural pathways.

A direct *link* can be established between a number of mechanoreceptors in the skin and well-defined areas in the brain. The *location* of a stimulus is the set of *active* neural pathways leading to specific brain areas (i.e., *maps*) encoding neural information originating from mechanical transduction. Since for each stimulus modality (such as high and slow frequency contact or temperature) a corresponding set of brain maps exists, the location of a stimulus can be defined also as the set of active map areas in the brain that are innervated by active neural pathways.

Topographic relationships between mechanoreceptors and brain maps are mediated by *receptive fields* of sensory neurons: a number of neural pathways is activated as a consequence of a stimulus possibly detected by *many* mechanoreceptors. From a morphological perspective, a receptive field is a small region of the skin that is innervated by a number of mechanoreceptors: it covers exactly the area of the skin that, if stimulated, is responsible for activating a number of neural pathways. Depending on the number of mechanoreceptors innervating sensory neurons, receptive fields can have *varied* amplitude. In particular, the density of mechanoreceptors throughout the skin is *not* uniform: the higher the density, the smaller the receptive field. This is motivated by cognitive processes related to use, required dexterity and evolution. For instance, fine grained tactile resolution is needed primarily in hands for manipulating objects, whereas the torso does not require the same resolution, since - usually - knowing that a contact occurred in the torso (without precise localization of the contact point) is enough to take immediate motor decisions. The density of mechanoreceptors determines the quality attained in resolving the details of stimuli in the corresponding skin areas. Differences in mechanoreceptors *resolution* are reflected in the central nervous systems, because of the mapping between mechanoreceptors, receptive fields, neural pathways and higher level maps, which are created by the topographic arrangement of afferent neural pathways. Specifically, larger portions of brain topographic maps correspond to skin areas with higher density, whereas smaller portions of topographic maps are related to skin areas with low density of tactile elements.

Because of the morphology associated with receptive fields, adjacent skin areas (i.e., skin *patches*) may overlap, because of the multiple way in which mechanoreceptors innervate sensory neurons. This is implicitly aimed at increasing robustness and fault-tolerance, and in general to obtain information suitable to detect specific patterns in sensory data. As a matter of fact, skin patches are especially arranged to perform certain operations, such as detecting spatial contrast during contact, and in particular edges (a computational model able to simulate a similar mechanism in the field of vision has been introduced in [26]).

From this short discussion, it emerges that, in order to design a comprehensive architecture for large-scale tactile data representation in robots, issues related to taxels location, mutual displacement, functional maps between taxels and their cognitive representation, density, varying resolution as well as functional processing abstraction must be seriously

taken into account.

III. Towards an Artificial Somatosensory Map

This Section describes the main ideas underlying the proposed model for representing artificial somatosensory maps. Assuming that patches of robot skin have been fixed over robot surfaces, obtaining a somatosensory map involves a two-step process: (i) taxels spatial calibration and (ii) functional mapping. In the following paragraphs, the actual representation infrastructure is discussed in its many facets.

A. Calibrating the Spatial Arrangement of Skin Taxels

The problem of robot skin calibration has been defined in [2] as *the automated process of determining the location of taxels with respect to a known reference frame, after the taxels have been actually fixed on a robot body link*. Skin calibration can be modelled as a maximum-likelihood mapping problem [25], [1], which determines taxel poses minimizing a properly defined functional. The robot skin is modelled as a *discrete* 3D surface S, a *mesh* made up of a number of s triangles $T_{S,1},...,T_{S,s}$ [21]. Specifically, *vertices* represent taxel poses expressed with respect to a common reference frame, whereas *edges* encode information about the relative displacement of two nearby taxels: both vertices and edges are estimated by the calibration process. Referring to the terminology introduced in [10]:

- $\mathbf{t}$ is a vector $(\mathbf{t}_1,...,\mathbf{t}_t)^T$ representing the estimated poses $\mathbf{t}_i$ of the $t = s+2$ taxels to calibrate, i.e., a *configuration*.
- δ_{ji} describes a measured displacement between poses $\mathbf{t}_i$ and $\mathbf{t}_j$. In particular, it refers to an actual observation of taxel j with respect to taxel i.
- Ω_{ji} is the *information* matrix modelling the likelihood associated with the measurement δ_{ji}.
- $h_{ji}(\mathbf{t})$ is the measurement model that computes an ideal observation of δ_{ji} w.r.t. the current estimate of $\mathbf{t}$.

The goal of skin calibration is to find the configuration $\mathbf{t}^*$ maximizing the likelihood of observations δ_{ji}, properly weighted by the corresponding Ω_{ji}, which corresponds to minimizing the error associated with each observed displacement:

$$e_{ji} = h_{ji}(\mathbf{t}) - \delta_{ji}.$$

Assuming that observations are characterized by Gaussian error, the negative log-likelihood of an observation h_{ji} is given by:

$$\begin{aligned} H_{ji}(\mathbf{t}) &= \frac{1}{2}\left[h_{ji}(\mathbf{t}) - \delta_{ji}\right]^T \Omega_{ji}\left[h_{ji}(\mathbf{t}) - \delta_{ji}\right] \\ &\propto e_{ji}(\mathbf{t})^T \Omega_{ji} e_{ji}(\mathbf{t}). \end{aligned}$$

If the observations are pairwise independent, the negative log-likelihood of the configuration $\mathbf{t}$ is

$$H(\mathbf{t}) = \frac{1}{2}\sum_{\langle j,i\rangle\in\Delta} e_{ji}(\mathbf{t})^T \Omega_{ji}(\mathbf{t}) e_{ji}(\mathbf{t}),$$

where Δ is the set of coupled indexes for which an observation δ_{ji} has been acquired. The goal configuration $\mathbf{t}^*$ can be found by minimizing $H(\mathbf{t})$, i.e.,

$$\mathbf{t}^* = \arg\min_{\mathbf{t}} \quad H(\mathbf{t}) \tag{1}$$

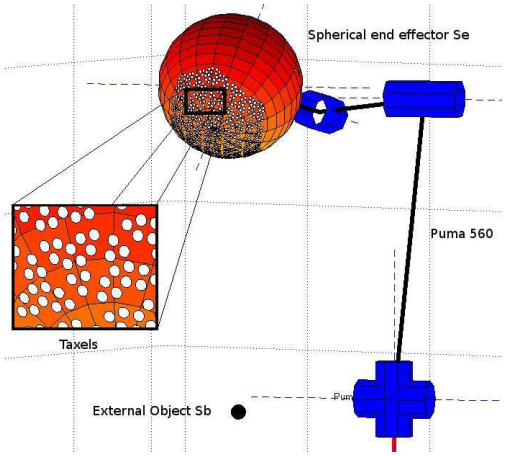

Fig. 2. The *red* sphere is kept in contact during movement with an *external object*: transducers fixed on the sphere are sequentially activated to obtain taxels estimated poses and displacements.

In literature, many algorithms exist to efficiently solve this problem [1], retrieving either the exact solution [25] or an approximation [9], even on-line [10]. However, the need arises to obtain both estimated poses $\mathbf{t}$ and measured displacements δ_{ji} for elements in Δ. In [2], a technique for robot skin calibration has been introduced that is able to obtain a set of measurements δ_{ji} by keeping the robot in contact with an external object of known location thereby generate the required tactile stimuli by taxels activation (see Figure 2). These data are then used to solve Equation 1 by means of an off-line algorithm very similar to what has been presented in [9].

The outcome of the skin calibration process, namely a discrete 3D surface S whose vertices $\mathbf{t}_i$, with $i = 1,...,t$, represent estimated taxel poses, is to be represented in cognitive maps by means of a topographic arrangement.

B. Mapping Robot Skin to Artificial Brain Maps

This Section is aimed at describing the main ideas and the formal framework adopted to obtain artificial somatosensory maps from calibrated skin. The key idea is to use the theory of *Surface Parametrization* to obtain a flat 2D representation (i.e., an *analogue* to cognitive maps in the cortex) of the 3D calibrated skin mesh [27], [21], [12]. The use of such a theory is motivated since it allows to *topographically preserve taxels locations, displacements, density and proximity relationships in cognitive structures*.

In this work, a technique for obtaining *Natural Intrinsic Parameterizations* is exploited to meet these requirements. This family of algorithms [6] allows to obtain free boundary parameterizations able to (sub)optimally preserve a linear combination of usually contradicting desired properties, namely *conformality* (i.e., angles between curves in the discrete 3D surface are preserved in the 2D mesh) and

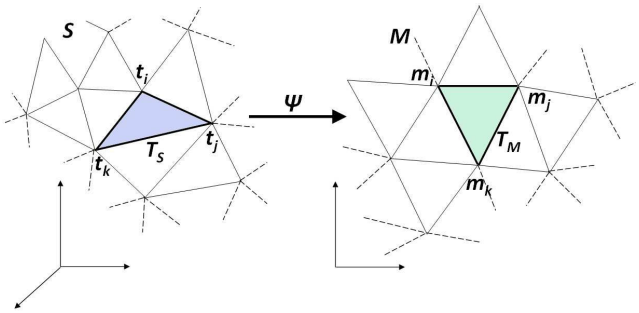

Fig. 3. Cognitive maps are discrete 2D surfaces isomorphic to robot skin.

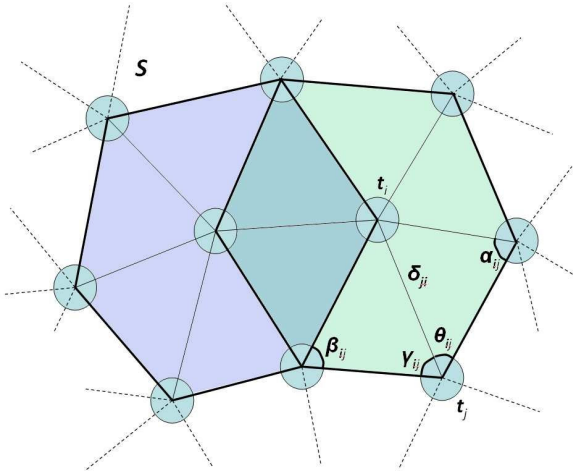

Fig. 4. The skin is modelled as a discrete surface in 3D made up of overlapping 1-rings.

authalicity (i.e., areas inscribed by edges in the original 3D mesh are preserved).

More formally, given a discrete 3D surface S (i.e., calibrated skin, possibly with *holes*), the goal is *to build a piecewise linear mapping* $\Psi : S \rightarrow M$ *between* S *and an isomorphic discrete 2D surface* M *(i.e., a cognitive map made up of* s *triangles* $T_{M,1},...,T_{M,s}$*) best preserving the intrinsic properties of* S (see Figure 3). In other words, for each $\mathbf{t}_i \in S$ a corresponding $\mathbf{m}_i \in M$ exists such that $\mathbf{t}_i = \Psi^{-1}(\mathbf{m}_i)$. Since there is no general way of flattening a discrete 3D surface onto a 2D plane, a number of distorsion measures E are usually introduced, which are defined as

$$E : \mathscr{S} \times \mathscr{S} \rightarrow R,$$

where $\mathscr{S}$ denotes the domain of generic discrete surfaces and R is a real number. Given S_1 and $S_2 \in \mathscr{S}$, it is evident that a minimum value for the distorsion measure $E(S_1,S_2)$ exists when S_1 and S_2 coincide (i.e., no distorsion), and therefore E can be treated as an *energy* functional. As a consequence, the initial problem can be reformulated as *determining an isomorphic discrete 2D surface* M *such that a properly defined energy functional* $E(S,M)$ *is minimal*. A discrete 3D surface S can be developed in a number of overlapping *1-rings*, namely exagons made up of central taxels $\mathbf{t}_i$ and surrounding taxels $\mathbf{t}_j$ (see Figure 4). For all the 1-rings in S, for a given distorsion measure E, and for each boundary taxel $\mathbf{t}_j$ *a priori* associated with an element of *known* location $\mathbf{m}_j$ in M (i.e., the boundary of M is *fixed*), the condition for the corresponding 1-ring in M to be optimal (i.e., minimally distorted) is that

$$M = \arg\min_{\mathscr{M} \backsim S} \quad E(S,\mathscr{M}), \tag{2}$$

where $\mathscr{M} \backsim S$ denotes the set of all the parameterizations isomorphic to S. Equation 2 is satisfied by imposing that, for each $\mathbf{m}_i \in M$, the energy value of the distorsion measure is at its minimum:

$$\frac{\partial E}{\partial \mathbf{m}_i} = 0. \tag{3}$$

Valid energy functionals must be characterized by: (i) *invariance* to both rotation and translation of surfaces; (ii) *conditional continuity* as the discrete 3D surface approximates a continuous one; (iii) *additivity* with respect to discrete surfaces. In order to meet these requirements, it has been demonstrated that energy functionals must assume a well-defined form, i.e., they must be represented as *linear* combinations of *Minkovsky* functionals [22], as follows:

$$E = \lambda_1 E^a + \lambda_2 E^\chi + \lambda_3 E^p. \tag{4}$$

In Equation 4, E^a represents functionals able to preserve angles, thereby leading to conformal mappings (imposing $\lambda_2 = \lambda_3 = 0$), E^χ stands for functionals suitable to preserve areas, i.e., the authalic component (with $\lambda_1 = \lambda_3 = 0$), whereas E^p is related to boundary conditions, i.e., the *perimeter* for discrete 3D surfaces. Minimizing E as defined in Equation 4 is expected to produce a cognitive map M that optimally represents in terms of angles and areas distorsion the robot skin surface S, thereby meeting functional requirements envisaged in Section II.

Traditionally, E^a has been associated with a specific functional, namely the *Dirichlet* energy of the map Ψ, defined in the continuous case[1] as

$$E_D(\Psi) = \frac{1}{2}\int_M |\nabla\Psi|^2.$$

In [21] a derivation for discrete surfaces is reported, which models the Dirichlet energy as the sum of all the piecewise linear energies related to corresponding triangles in S and M. Given two triangles $T_s \in S$ and $T_m \in M$ such that $T_s = \Psi_{sm}^{-1}(T_m)$, then the Dirichlet energy of Ψ_{sm} is given by,

$$E_D(\Psi_{sm}) = \frac{1}{4}\sum_{\langle j,i\rangle \in \Delta_{T_s}} \cot\alpha_{ij}|\mathbf{m}_i - \mathbf{m}_j|^2,$$

where Ψ_{sm} is the mapping between triangles T_s and T_m, Δ_{T_s} contains three elements, namely the three edges δ_{ji} defining T_s, α_{ij} are the angle opposed to the links δ_{ji} connecting taxels $\mathbf{t}_i$ and $\mathbf{t}_j$, whereas $\mathbf{m}_i$ and $\mathbf{m}_j$ are elements in M of *unknown* location corresponding to taxels $\mathbf{t}_i$ and $\mathbf{t}_j$ in S (see Figure 4). As a consequence, the term E^a for the single 1-ring r can be computed as the sum of the Dirichlet energy

[1]The use of Ψ and M for, respectively, the mapping and the parameterization is unappropriate, since they refer to discrete surfaces.

over all the involved triangles, decreased by energy terms for overlapping edges:

$$E^a = \sum_{\langle j,i\rangle \in \Delta_r} \cot \alpha_{ij} |\mathbf{m}_i - \mathbf{m}_j|^2. \quad (5)$$

Equation 5 holds for any 1-ring r the discrete surface S is made up of. According to Equation 3, discrete conformal maps for 1-rings can be obtained by computing the minimum of the Dirichlet energy as defined in Equation 5, w.r.t. the median parameter $\mathbf{m}_i$:

$$\frac{\partial E^a}{\partial \mathbf{m}_i} = \sum_{j:\langle j,i\rangle \in \Delta_r} (\cot \alpha_{ij} + \cot \beta_{ij})(\mathbf{m}_i - \mathbf{m}_j) = 0, \quad (6)$$

where α_{ij} and β_{ij} are the angles opposed to δ_{ji} on both sides. It is then straightforward to obtain the global energy associated with conformal maps of the surface S summing up all the contributions from related 1-rings[2]. However, it is worth noticing that, since coefficients in Equation 6 depend only on angles between edges of S, minimizing this functional leads to angle-preserving maps. Furthermore, as described in [11], since E^a is related to the determinant of the *first* fundamental form, it is indeed an implicit measure of how much an area is distorted.

On the other hand, E^χ has be associated with the *Euler* characteristic, which is strictly related to the determinant of the *second* fundamental form [6]. Again, in case of 1-rings, E^χ can be expressed as function of taxels locations, corresponding parameterizations and proper angles of S (see Figure 4):

$$E^\chi = \sum_{j:\langle j,i\rangle \in \Delta_r} \frac{\cot \alpha_{ij} + \cot \beta_{ij}}{|\mathbf{t}_i - \mathbf{t}_j|^2} (\mathbf{m}_i - \mathbf{m}_j)^2. \quad (7)$$

Equation 7 holds for any 1-ring r belonging to surface S. Combining Equations 3 and 7, discrete authalic maps can be obtained by computing the minimum of the energy E^χ w.r.t. the median parameter $\mathbf{m}_i$:

$$\frac{\partial E^\chi}{\partial \mathbf{m}_i} = \sum_{j:\langle j,i\rangle \in \Delta_r} \frac{\cot \alpha_{ij} + \cot \beta_{ij}}{|\mathbf{t}_i - \mathbf{t}_j|^2} (\mathbf{m}_i - \mathbf{m}_j) = 0. \quad (8)$$

As in the previous case, the global energy associated with authalic maps can be computed summing up all the contributions from 1-rings. In this case, coefficients in Equation 8 only depend on local areas of the orginal 3D surface: as a consequence, minimizing E^χ leads to area-preserving maps, which is not surprising given the tight relationships with the second fundamental form.

Finally, it is worth noticing that energy functionals related to E^p are still subject of open research issues. Recently, few papers appeared in literature aiming at relaxing the fixed boundary condition assumed to define Equation 2 exploiting the linearity associated to Minkovsky functionals [14], [12]: practice suggests that allowing free boundaries leads to maps whose overall distorsion metric is more homogeneous and qualitatively acceptable. Although exploited in the current implementation, this issue is not further investigated in the paper.

[2]This is outside the scope of the paper. The reader is referred to [21].

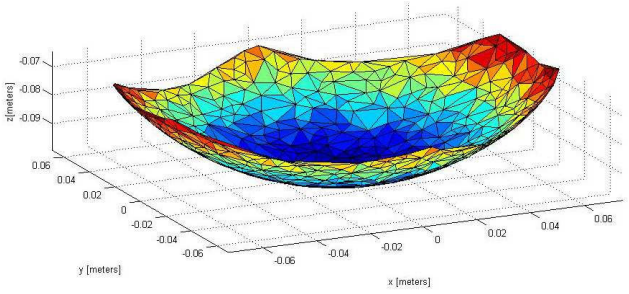

Fig. 5. The skin discrete 3D surface associated with the bottom part of the calibrated sphere S_e.

If a discrete 3D surface S representing calibrated robot skin is parameterized using a cognitive map M obtained as the minimization of an energy functional defined as in Equation 4, it is expected that elements $\mathbf{m}_i \in M$ represent a topographic arrangement of taxels $\mathbf{t}_i$ preserving density, displacements and proximity relationships.

IV. Experimental Validation

As described in Section III-A, the proposed framework has been validated in a simulated scenario. A spherical body S_e is fixed on the end effector of an anthropomorphic arm. Taxels $\mathbf{t}_i$ are mounted over S_e (see the *red* sphere in Figure 2), and are activated in sequence by the physical interaction between S_e and another small *black* sphere S_b whose pose is known with respect to an external reference frame. The physical contact is maintained using a compliance motion control law described in [2]. As long as S_e is moved around S_b, initial estimates for both taxel poses $\mathbf{t}_i$ and their mutual displacements δ_{ji} are recovered. Then, the minimization process required to solve Equation 1 is carried out, thereby obtaining a maximum-likelihood estimate of taxels configuration.

The simulation environment exploits the well-known Robotics Toolbox under MATLAB / Simulink [4]. S_e is a sphere of radius $0.1m$ whose material is *elastic* and *deformable*. In the bottom part of the sphere around 500 taxels are located, with a mean distance between them of around $5mm$. According to the design proposed in [18], taxels are arranged in triangular patterns, and are modelled as *ideal capacitive transducers* of $2mm$ radius that can measure the exact exerted force. Differently from the sphere mounted on the robot's end effector, S_b is not deformable and its radius is sensibly shorter, i.e., $0.01m$.

Assuming to calibrate the sphere S_e, Figure 5 shows the result of the minimization process associated with the solution of Equation 1, if measurements are perturbed by $N(0m, 1mm^2)$. In particular, vertices of the triangular structure correspond to taxel poses $\mathbf{t}_i$, whereas edges represent estimated distances δ_{ji} between taxels. As a matter of fact, S_e is a discrete 3D surface that can be represented using a flat 2D map.

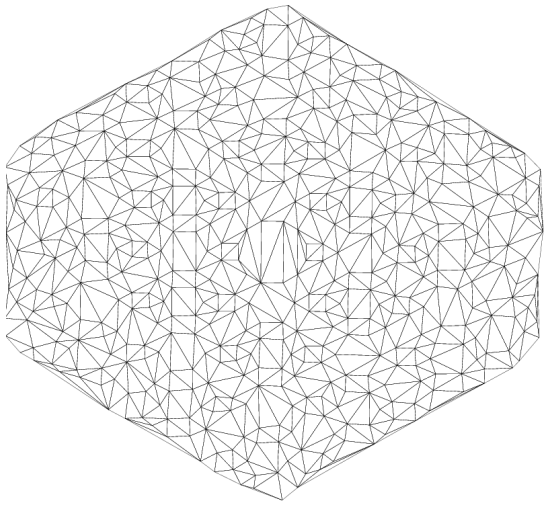

Fig. 6. The isomorphic discrete 2D surface M_e representing S_e.

The corresponding somatosensory map M_e is obtained using the technique described in Section III-B, assuming an intrinsic parameterization with free boundaries (see Figure 6). As it can be noticed, a certain level of distorsion is introduced, especially at the border. However, corners associated with the original surface M_e are clearly visible also in the corresponding S_e. The configuration of taxels originating from the calibration process is preserved in its general shape by elements $\mathbf{m}_i$ (in terms of areas and angles) as well as in proximity relationships and mutual displacements.

V. Conclusions

This paper introduces a framework for representing tactile information that is inspired by similar mechanisms in humans. After having fixed taxels over the robot surface, their spatial arrangement is first retrieved through a calibration process, and then mapped to a 2D surface preserving *at best* in the sense of Equation 3 the mutual displacement between taxels. The exploited mathematical framework allows to establish an isomorphic mapping between a taxel in the tactile map and the corresponding position in 3D space, which is a desirable property for controlled contact tasks. Issues related to computational requirements for an effective use of tactile maps by high level cognitive tasks is not explicitly addressed in this paper. However, inspired by the work presented in [8], [3], [7] a hierarchical tactile representation framework is subject of on-going investigation.

References

[1] W. Burgard, C. Stachniss, G. Grisetti, B. Steder, R. Kuemmerle, C. Dornhege, M. Ruhnke, A. Kleiner, J.D. Tardos. A Comparison of SLAM Algorithms Based on a Graph of Relations. In *Proc. of the 2009 IEEE/RSJ Int.l Conf. on Intelligent Robots and Systems (IROS)*, St. Louis, MO, USA, October 2009.

[2] G. Cannata. S. Denei and F. Mastrogiovanni. Towards Automated Self-Calibration of Robot Skin. In *Proc. of the 2010 IEEE Int.l Conf. on Robotics and Automation (ICRA)*, Anchorage, Alaska, USA, May 2010.

[3] Y. Chen. A Motor Control Model Based on Self-Organizing Feature Maps. *Ph.D. Dissertation*, University of Mariland, 1997.

[4] P.I. Corke. MATLAB Toolboxes: Robotics and Vision for Students and Teachers. In *IEEE Robotics and Automation Magazine*, vol. **14**(4):16–17, December 2007.

[5] R.S. Dahiya, G. Metta, M. Valle and G. Sandini. Tactile Sensing: from Humans to Humanoids. In *IEEE Trans. on Robotics*, vol. **26**(1), pp. 1–20, 2010.

[6] M. Desbrun, M. Meyer and P. Alliez. Intrinsic Parametrizations of Surface Meshes. In *Computer Graphics Forum*, vol. **21**(3), pp. 209–218, September 2002.

[7] K.A. Doherty, R.G. Adams and N. Davey. Hierarchical Growing Neural Gas. In *Proc. of the Seventh Int.l Conf. on Adaptive and Natural Computing Algorithms (ICANNGA)*, Coimbra, Portugal, March 2005.

[8] B. Fritzke. A Growing Neural Gas Network Learns Topologies. In G. Tesauro, D.S. Touretzky and T.K. Leen (Eds.) *Advances in Neural Information Processing Systems 7*, pp. 625-632, MIT Press, 1995

[9] G. Grisetti, S. Grzonka, C. Stachniss, P. Pfaff and W. Burgard. Efficient Estimation of Accurate Maximum Likelihood Maps in 3D. In *Proc. of the 2007 IEEE/RSJ Int.l Conf. on Intelligent Systems and Robots (IROS)*, San Diego, CA, USA, October 2007.

[10] G. Grisetti, D. Lodi Rizzini, C. Stachniss, E. Olson and W. Burgard. Online Constraint Network Optimization for Efficient Maximum Likelihood Mapping. In *Proc. of the 2008 IEEE Int.l Conf. on Robotics and Automation (ICRA)*, Pasadena, CA, USA, May 2008.

[11] A. Gray. Modern Differential Geometry of Curves and Surfaces. Second Edition, CRC Press, 1998.

[12] K. Hormann, B. Lvy and A. Shaffer. Mesh Parameterization: Theory and Practice. In *Proc. of the 2007 ACM Int.l Conf. on Computer Graphics and Interactive Techniques (SIGGRAPH*, San Diego, CA, USA, August 2007.

[13] E. Kandel, J.H. Schwartz and T.M. Jessell. Principles of Neural Science. Fourth Edition, McGraw-Hill, New York, 2000.

[14] Z. Karni, C. Gotsman and S.J. Gortler. Free Boundary Linear Parameterization of 3D Meshes in the Presence of Constraints. In *Proc. of the 2005 IEEE Int.l Conf. on Shape Modelling and Applications (SHI)*, Cambridge, MA, USA, June 2005.

[15] Y. Kuniyoshi, Y. Yorozu, Y. Ohmura, K. Terada, T. Otani, A. Nagakubo, T. Yamamoto. From Humanoid Embodiment to Theory of Mind. In *Embodied Artificial Intelligence*, pp. 202-218, Lecture Notes in Computer Science, Springer Berlin / Heidelberg, 2003.

[16] Y. Kuniyoshi and S. Sangawa, Early Motor Development from Partially Ordered Neural-Body Dynamics: Experiments with a Cortico-Spinal-Musculo-Skeletal Model. In *Biological Cybernetics*, vol. **95**, pp. 589-605, 2006.

[17] T. Kuriyama and Y. Kuniyoshi. Co-Creation of Human-Robot Interaction Rules through Response Prediction and Habituation / Dishabituation. In *Proc. of the 2009 IEEE Int.l Conf. on Intelligent Robots and Systems (IROS)*, St. Louis, MO, USA, October 2009.

[18] M. Maggiali. Artificial Skin for Humanoid Robots. Ph.D. Disseration, University of Genova, 2008.

[19] T. Noda, T. Miyashita, H. Ishiguro and N. Hagita. Super-Flexible Skin Sensors Embedded on the Whole Body, Self-Organizing Based on Haptic Interactions. In *Proc. of Robotics: Science and Systems IV*, Zurich, Switzerland, June 2008.

[20] L. Olsson, C.L. Nehaniv and D. Polani. From Unknown Sensors and Actuators to Actions Grounded in Sensorimotor Perceptions. In *Connection Science*, vol. **18**(2), 2006.

[21] U. Pinkall and K. Polthier. Computing Discrete Minimal Surfaces and Their Conjugates. In *Experimental Mathematics*, vol. **2**(1), pp. 15–36, 1993.

[22] L. Santalo. Integral Geometry and Geometric Probability. Addison-Wesley, 1976.

[23] W.D. Stiehl, L. Lalla, C. Breazeal. AA Somatic Alphabet Approach to Sensitive Skin for Robots. In *Proc. of the 2004 IEEE Int.l Conference on Robotics and Automation (ICRA'04)*, New Orleans, LO, USA, May 2004.

[24] P.M. Thompson, J.N. Giedd, R.P. Woods, D. MacDonals, A.C. Evans and A.W. Toga. Growth Patterns in the Developing Brain Detected by Using Continuum-Mechanical Tensor Maps. In *Nature*, vol. **404**, pp. 190-193, 2000

[25] S. Thrun, W. Burgard and D. Fox. Probabilistic Robotics. The MIT Press, 2005.

[26] G. Yu and J.J. Slotine. Visual Grouping by Oscillator Networks. In *IEEE Trans. on Neural Networks*, vol. **20**(12), pp. 1871–1884, 2009.

[27] W.L. Wilson. On Discrete Dirichlet and Plateau Problems. In *Numerische Mathematik*, vol. **3**, pp. 359–373, 1961.